Estimating heart shift and morphological changes during minimally invasive cardiac interventions

Cristian A. Linte[a,b], Mathew Carias[c], Daniel S. Cho[a,b], Danielle F. Pace[a,b], John Moore[a], Chris Wedlake[a], Daniel Bainbridge[d,f], Bob Kiaii[e,f] and Terry M. Peters[a,b,c,f]

[a]Imaging Research Laboratories, Robarts Research Institute,
[b]Biomedical Engineering Graduate Program, University of Western Ontario,
[c]Department of Medical Biophysics, University of Western Ontario,
[d]Division of Anesthesia, University of Western Ontario,
[e]Division of Cardiac Surgery, University of Western Ontario,
[f]Canadian Surgical Technologies and Advanced Robotics (CSTAR),
London ON Canada.

ABSTRACT

Image-guided interventions rely on the common assumption that pre-operative information can depict intra-operative morphology with sufficient accuracy. Nevertheless, in the context of minimally invasive cardiac therapy delivery, this assumption loses ground; the heart is a soft-tissue organ prone to changes induced during access to the heart and especially intracardiac targets. In addition to its clinical value for cardiac interventional guidance and assistance with the image- and model-to-patient registration, here we show how ultrasound imaging may be used to estimate changes in the heart position and morphology of structures of interest at different stages in the procedure. Using a magnetically tracked 2D transesophageal echocardiography transducer, we acquired in vivo images of the heart at different stages during the procedural workflow of common minimally invasive cardiac procedures, including robot-assisted coronary artery bypass grafting, mitral valve replacement/repair, or model-enhanced US-guided intracardiac interventions, all in the coordinate system of the tracking system. Anatomical features of interest (mitral and aortic valves) used to register the pre-operative anatomical models to the intra-operative coordinate frame were identified from each dataset. This information allowed us to identify the global position of the heart and also characterize the valvular structures at various peri-operative stages, in terms of their orientation, size, and geometry. Based on these results, we can estimate the differences between the pre- and intra-operative anatomical features, their effect on the model-to-subject registration, and also identify the need to update or optimize any pre-operative surgical plan to better suit the intra-operative procedure workflow.

Keywords: Minimally Invasive Cardiac Procedures, Data Integration for the Clinic/OR, Pre-operative Procedure Planning, Peri-operative Workflow, Intra-operative Guidance, Localization and Tracking Technologies.

1. INTRODUCTION

The quest for less invasive alternatives to conventional cardiac surgery and therapy techniques has been motivated by the necessity to reduce patient morbidity, recovery time, and health care costs. During the past decade, the recognition of the significant advantages of minimizing surgical trauma by reducing incision size and eliminating tissue exposure have resulted in a substantial increase in the number of minimally invasive cardiac surgical procedures being performed. These benefits have included less pain, shorter hospital stays, faster return to normal activities and improved cosmesis.[1–4] Concurrently, improvements in surgical instrumentation, perfusion technology and visualization platforms have facilitated these advances to the point that these minimally invasive approaches have become the standard of care at certain institutions worldwide due to their excellent results.[5]

Further author information:
Cristian A. Linte (E-mail: clinte@imaging.robarts.ca)
Terry M. Peters (E-mail: tpeters@imaging.robarts.ca)
Imaging Research Labs, Robarts Research Institute: 100 Perth Dr., P.O.Box: 5015, London ON N6A 5K8 Canada.

Medical Imaging 2010: Visualization, Image-Guided Procedures, and Modeling, edited by Kenneth H. Wong, Michael I. Miga, Proc. of SPIE Vol. 7625, 762509 · © 2010 SPIE · CCC code: 1605-7422/10/$18 · doi: 10.1117/12.845579

Downloaded From: http://spiedigitallibrary.org/ on 12/17/2012 Terms of Use: http://spiedl.org/terms

As an alternative to conventional therapy approaches, performing interventions on the beating heart is considered to be the ultimate and least invasive cardiac therapy delivery technique. The challenge nevertheless, lies within the ability to provide the interventionalist with a clear and intuitive display of the surgical field to enable target identification and surgical tool manipulation with sufficient accuracy and fidelity without compromising therapy delivery outcome.

For most of these procedures, in addition to the intra-operative visualization achieved using various medical imaging modalities, a pre-operative planning stage is often involved. In the case of CABG procedures, for example, a pre-operative computer tomography (CT) scan is used to assess patient candidacy for the robot-assisted procedure (i.e., the thorax anatomy of the patient allows the surgery to be performed using the surgical robot, ensuring the instruments can reach the heart without colliding with each other). Also based on the pre-operative dataset, the surgeon identifies the location of the target vessel - the left anterior descending (LAD) coronary artery, as well as the optimal location of the port incisions to ensure proper access to the regions of interest. Moreover, often the target vessel - the LAD - cannot be identified intra-operatively and the surgeon must predict where the same target would be located based on the pre-operative image information.

Besides the CABG procedures, other novel minimally invasive techniques such as the ones reported in our laboratory[6] using model-enhanced US guidance,[7] involve an image-to-patient registration step, where real-time intra-operative US imaging is augmented with pre-operative anatomical models of the heart, using a feature-based registration. A similar approach is presented by Ma *et al.*,[8] where they use a feature-based approach to register pre-operative data to the intra-operative US images at a single stage before the procedure. For both of these scenarios, the planning and visualization environment must adequately resemble the real surgical field to allow proper surgical navigation, and hence a clinically adequate alignment between the pre-operative models used in therapy planning and the intra-operative information used in therapy delivery is expected. Nevertheless, one has to bare in mind that the morphology of these features as depicted pre-operatively will differ to some extent from those identified intra-operatively, simply due to a slightly different position of the subject, as well as changes induced during the workflow of the procedure itself. Hence, any information with regards to the changes in position, orientation and intrinsic morphology of these features is critical for either updating a pre-operative plan or provide an initial image-to-patient registration.

This work is therefore motivated by both our current developments on model-enhanced US intracradiac surgical navigation, as well as a parallel project aimed on optimizing post placement and surgical planning for robot-assisted CABG procedures. Here we focus on estimating the changes that occur in the heart between the pre- and various peri- and intra-operative stages, not only from a global positioning perspective, but also from a selected-feature morphological perspective, for robot-assisted CABG procedures in patients as well as for off-pump intracardiac procedures in porcine models with access inside the beating heart achieved via the Guiraudon Universal Cardiac Introducer® (GUCI). All human data presented here was acquired following approval of the Research Ethics Board of the University of Western Ontario and patient consent. Moreover, all animal experiments described in this study were approved by the Animal Care and Use Committee of The University of Western Ontario and followed the guidelines of the Canadian Council on Animal Care.

2. METHODOLOGY

In order to estimate the changes in global position and morphology of the heart during the procedure workflow of common minimally invasive interventions, we rely on features of the heart that are available in the pre-operative CT or MR images and that can also be readily obtained from real-time intra-operative US images of the subject's heart acquired at the various stages of the procedural workflow.

Here we use the mitral and aortic valves as the features of interest and assess their global movement and morphological changes during the intra-procedure workflow. These features are not only involved in the image- or model-to-patient registration previously described using both patient and porcine image data, but they are also key features in another registration technique currently under development in our laboratory that uses the coronary ostia and left ventricular apex in addition to the two valves to map the pre-operative location of the left anterior descending coronary vessel into the intra-operative environment for improved planning and guidance of robot-assisted CABG procedures.

Downloaded From: http://spiedigitallibrary.org/ on 12/17/2012 Terms of Use: http://spiedl.org/terms

We are interested in two types of changes in heart location and geometry induced during a specific procedural workflow: overall movement of the heart - a measure of the magnitude and direction of how much the heart itself shifts during the procedure; and morphological changes of the features of interest - a measure of the geometrical variations of the features of interest during the workflow. The morphological changes are also a measure of the variability associated with the identification and segmentation of the valvular features, which, in turn, contributes to the uncertainty of any registration algorithm that involves those features.

2.1 Minimally Invasive Procedure Workflow

While all minimally invasive cardiac interventions that involve procedure planning require a similar analysis, in this paper we focus on two procedures: off-pump robot-assisted CABG and off-pump model-enhanced US guided procedures performed via GUCI-based intracardiac access. In addition, the analysis shown here is preliminary and it is based on two image datasets from porcine subjects that have undergone GUCI-based procedure and four patient image datasets who have undergone robot-assisted CABG procedure intervention.

2.1.1 Direct-access Off-pump Intracardiac Interventions via GUCI

Unlike some epicardial procedures which can be performed off-pump, such the one described above, most intracardiac procedures, including those performed under minimally invasive conditions, are carried out on the empty, arrested heart. Reduced invasiveness is achieved by entering the thoracic cavity via smaller incisions with reduced tissue exposure, usually using a lateral minithoracotomy. Together with our surgical collaborators, we have expanded on this approach; using the GUCI for off-pump intracardiac access in porcine models, we have demonstrated how model-enhanced US guidance and surgical instrument tracking can be used to position a prosthetic mitral valve and a septal defect repair patch onto the native mitral annulus and fossa ovalis, respectively, in live porcine subjects. Given that an adequate registration of the pre-operative models to the intra-operative imaging environment is required due to lack of direct intracardiac visualization, the features used for registration and any changes they undergo during the procedure need to be properly documented.

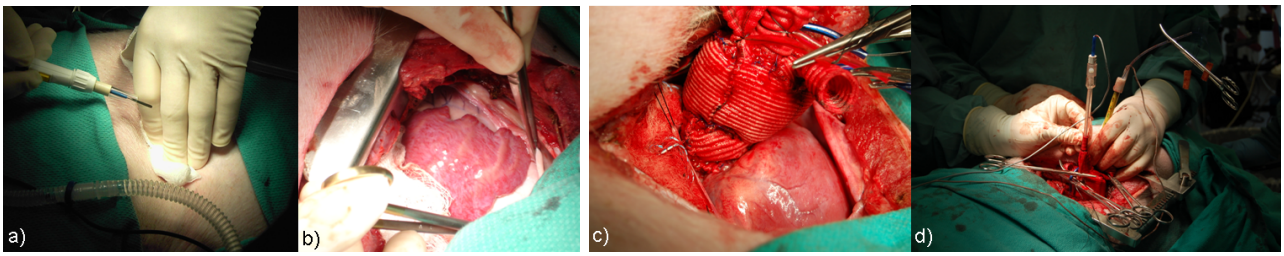

Figure 1. Peri-operative workflow stages associated with the GUCI-based intracardiac interventions: a) before opening chest; b) after minithoracotomy; c) after intracardiac access; d) during procedure.

After anesthesia, and mechanical dual-lung ventilation, (stage 1), the heart is accessed via a minithoracotomy and the pericardial sac is opened for access to the chamber of interest (stage 2). The GUCI is then attached to the left or right atrial appendage and the surgical instruments needed for the procedure are inserted inside the chamber via the ports of the GUCI (stage 3) (**Fig. 1**).

2.1.2 Robot-Assisted Coronary Artery Bypass Graft Interventions

Robot-assisted CABG procedures typically involve three peri-operative stages. Initially, the patient is anesthetized, with both lungs mechanically ventilated, and positioned slightly in the right lateral decubitus position (stage 1). This stage closely resembles the pre-operative imaging stage when the patient's heart is imaged in the same position and under similar breathing conditions, but under no anesthesia; hence the cardiac anatomy and morphology are thought to be very similar at these two stages. The left lung is then deflated to enable access to the heart (stage 2), while the patient undergoes single lung ventilation, followed by CO_2 chest wall insufflation (stage 3) at a target pressure of 10 cm H_2O.

Downloaded From: http://spiedigitallibrary.org/ on 12/17/2012 Terms of Use: http://spiedl.org/terms

2.2 Data Acquisition

2.2.1 Pre-operative Image Acquisition

For the RA-CABG procedures, a high-resolution pre-operative CT scan (64 Slice LightSpeed VCT, General Electric, Milwaukee, WI, USA) was acquired as part of the routine pre-operative imaging for candidacy assessment. Since x-ray contrast was used for the pre-operative scans, the images also provided accurate information about the location of the major blood vessels, including the coronary arteries. Geometric models of major heart structures can be constructed using existing techniques previously developed in our laboratory.[9]

For the GUGI-based intracardiac model-enhanced US guided procedures, a set of 20 high resolution (1.09 x 1.09 x 2.0 mm^3) ECG-gated MR volumes of a porcine subject's heart was acquired throughout the cardiac cycle. A pre-operative surface model was constructed from the mid-diastole volume,[10] consisting of the left ventricular myocardium (LV), left atrium (LA), right atrium and ventricle (RA/RV), and the mitral (MVA) and aortic valve annuli (AVA). For procedure guidance, a dynamic cardiac model may be obtained by animating the mid-diastolic model throughout the cardiac cycle using motion information extracted via non-rigid image registration[9] and synchronizing it with the ECG signal; however, for the purpose of this work, the mid-diastolic information is sufficient.

2.2.2 Peri-operative Image Acquisition

For both procedures the image acquisition was repeated at each stage of the peri-operative workflow. All data processing and analysis was performed off-line, after the procedures were completed.

In order to track the cardiac features of interest during the peri-operative workflow of the robot-assisted CABG procedures, we employed real-time transesophageal echocardiograpy (TEE). 2D US images were acquired using an Agilent Technologies (Model No.: 21369A) TEE transducer (Agilent Technologies, Canada). The probe was modified by embedding a 6 degree-of-freedom (DOF) NDI Aurora magnetic sensor coil (Northern Digital Inc., Waterloo, Canada) inside the encasing of the transducer and calibrated using the Z string technique,[11,12] enabling its spatial tracking. The magnetic field generator was located underneath the patient's heart, under the operating table (**Fig. 2**).

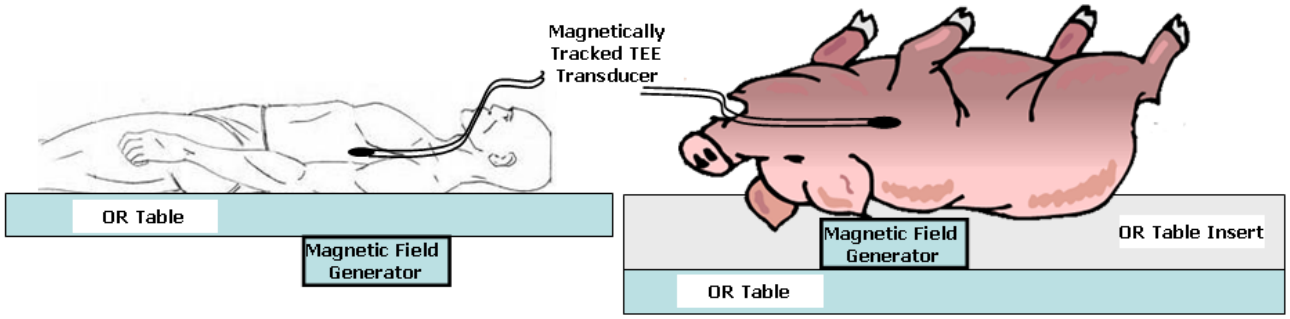

Figure 2. Intra-operative setup of the a) patient during image acquisition prior to the robot-assisted CABG procedure; and b) porcine subject prior to the GUCI-based off-pump intracardiac interventions.

In addition to spatial tracking, all images were acquired using ECG gating; the real-time US video feed was "frozen" at the 75% after the R-R interval, corresponding to the mid-diastole time point. The mitral valve was imaged via a series of 6-10 mid-esophageal four-chamber acquisitions at 20° angular increments. The aortic valve was imaged using a $180° \pm 10°$ long axis view and a 30° short axis view.

A similar acquisition protocol was used for the *in vivo* porcine cardiac image acquisition during the GUCI-based minimally invasive off-pump interventional workflow. However, instead of using the integrated magnetically tracked TEE probe, we used a similar transducer onto which the magnetic sensor coil was rigidly attached on the outside, similar to our previous work. Also, the field generator was located inside a mattress insert placed

Downloaded From: http://spiedigitallibrary.org/ on 12/17/2012 Terms of Use: http://spiedl.org/terms

underneath the pig on the operating table (**Fig. 2**). The mitral and aortic valves were imaged at $10 - 20°$ angular increments, however difficulties were encountered during the aortic valve image acquisition due to its obstruction by features belonging to the respiratory system.

2.2.3 Cardiac Feature Identification

The main advantage of the tracked image acquisition is the ability to interactively select features of interest in the image dataset at different times during the workflow, and display them relative to each other in the same coordinate system. As a result, all 2D image fans are inserted into the 3D volume according to their spatial stamp recorded by the tracking system.

Following image acquisition, all data processing was performed off-line. The 2D images were then reviewed by an experienced echocardiographer to identify the features of interest using a custom-developed interactive tool similar to the TomTec 4D MV-Assessment (TomTec Imaging Systems GmbH, Germany) commercially available software. Our custom-developed tool enables the user to visualize each of the acquired 2D US images and interactively select points corresponding to the structure of interest (i.e., each valve annulus is segmented by identifying the annular end points as seen on the incrementally acquired 2D images) (**Fig. 3**).

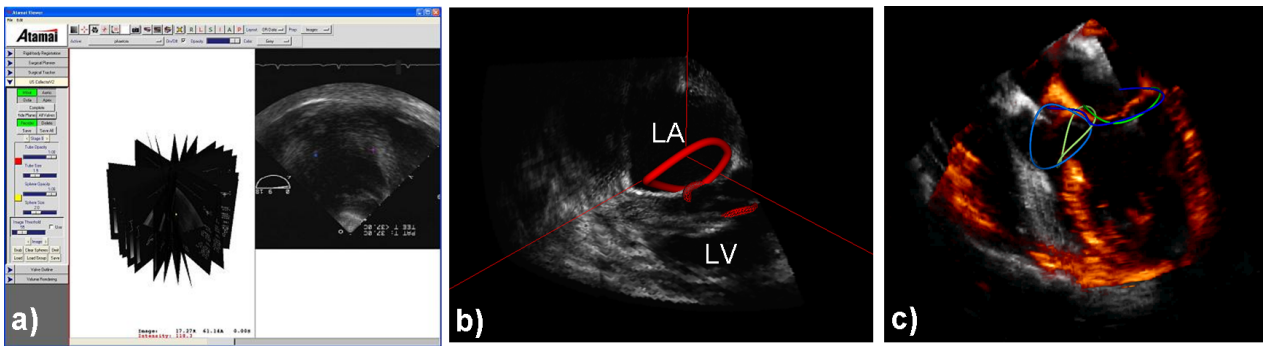

Figure 3. a) Screen shot showing the US image collection and analysis tool used to extract the features of interest (b) from the peri-operatviely acquired US images; c) Peri-operative US images at two different stages in the workflow showing the segmented mitral and aortic valve annuli.

The selected points were then transfered into the 3D coordinate system according to the spatial stamp of the 2D US fan they belonged to. The mitral and aortic annuli are represented by a series of 3D points which are then connected using a 3D spline, leading to a pair of continuous annuli. A similar tool was used to select the mitral and aortic annuli in the pre-operative CT and MR images, however, the process was facilitated by the superior image quality and 3D nature of the image datasets.

2.3 Data Analysis

2.3.1 Global Heart Movement

Since the procedures involve both pre- and peri-operative stages, and planning is performed on the pre-operative dataset, here we used the CT space coordinate system as the fixed global coordinate system. Moreover, since the subject was imaged in the same position and under the same physiological conditions both pre-operatively and during the first peri-operative stage (anesthetized, intubated, dual-lung ventilation), and assuming that no major changes were induced by the anesthesia, then a registration of the images based on the homologous features enabled us to determine the transform between the intra-operative coordinate system (i.e., the coordinate system of the tracking space) and that of the CT space. We simply performed an annulus-based registration using the intra-operative MVA and AVA as the moving features and the homologous pre-operative annuli as the fixed features.

The global motion of the heart was estimated according to the change in position of the mitral and aortic valve annuli between successive stages in the procedural workflow. The displacement was determined based on

Downloaded From: http://spiedigitallibrary.org/ on 12/17/2012 Terms of Use: http://spiedl.org/terms

the locations of the centroid of the mitral and aortic valve annuli expressed as a vector quantity and characterized by displacement magnitude and direction. The movement between consecutive stages was expressed in the CT coordinate system with respect to the anterior-posterior (AP), superior-inferior (SI) and left-right (LR) axes of the body.

2.3.2 Morphological Feature Characterization

In addition to estimating the overall displacement of the features as a global measure of the position of the heart, we also characterized feature morphology in terms of annulus length and length of its principal axes, corresponding to the major and minor in-plane radii and polar radius, the latter being a measure of the out-of-plane properties. While the native valves are not exactly planar structures, especially the mitral valve which is often referred to as saddle-shaped, the aortic valve does exhibit a more planar behaviour.

The morphological feature characterization was performed within a local coordinate system characterized by a basis consisting of three orthogonal unit vectors. The basis was identified using principal component analysis and eigenvalue decomposition of the covariance matrix of each valve annulus. The eigenvalues are a direct measure of the length of the in-plane and polar radii of each annular structure, which are directly proportional to the squared root of the eigenvalues in descending order, respectively. Furthermore, the direction of the principal axes of each feature were provided by the set of orthogonal eigenvectors, where the eigenvector corresponding to the lowest eigenvalue represented the normal of the orthogonal plane of best fit for each structure. Consequently, the lowest eigenvalue was a measure of the "spread" of the feature in the out-of-plane direction.

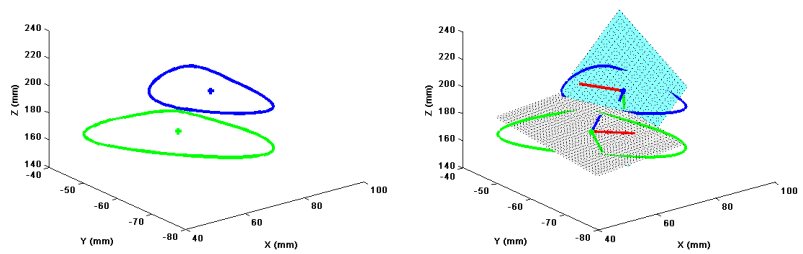

Figure 4. a) Figure showing the mitral (green) and aortic (blue) shown before chest opening in the porcine subject; b) Orthogonal best-fit plane shown, along with principal in-plane directions (red and green) and normal unit vector (blue).

Two other parameters were also estimated to provide a measure of local deformations within the heart: the inter-annular distance, represented by the distance between the centroids of the mitral and aortic annulus; and the relative annuli orientation, represented by the angle between the normals of the orthogonal plane of best fit of each annulus. Based on these parameters, one could assess whether significant local deformations occur between adjacent stages of the workflow, in which case a rigid registration algorithm may impose undesired limitations with respect to optimal procedure planning and guidance.

3. RESULTS

3.1 Overall Heart Movement

To evaluate the global motion of the heart during the peri-operative workflow, we first extracted the mitral and aortic annuli from each of the peri-operative US datasets. The peri-operative data was then registered into the same coordinate system as the pre-operative data using the homologous features at stage 1 (before incision in the case of GUCI-based intracardiac procedure or the dual-lung ventilation stage for the off-pump robot-assisted CABG procedure). **Table 1** includes a summary of the valvular and overall heart displacement across the three stages of the GUCI-based procedure.

For an intuitive graphical display, we show below the mitral and aortic valve annuli at consecutive stages (**Fig.5**), along with a generic model of the heart consisting of the left atrium and ventricle and positioned

Downloaded From: http://spiedigitallibrary.org/ on 12/17/2012 Terms of Use: http://spiedl.org/terms

Table 1. Summary of the overall heart and valve displacement between consecutive stages of an off-pump GUCI-based intracardiac intervention based on $N = 2$ porcine subjects. Stage 1: before minithoracotomy; Stage 2: After minithoracotomy; Stage 3: After GUCI attachment. Note that displacements are reported according to the left/right (L/R), anterior/posterior (A/P) and superior/inferior (S/I) directions, where positive displacements are measured toward the right, anterior and superior directions.

Workflow Stage	Overall Heart			Mitral Valve			Aortic Valve		
	L/R	A/P	S/I	L/R	A/P	S/I	L/R	A/P	S/I
Stage 1-2	17.9	-12.2	4.3	13.7	-6.8	4.2	22.2	-17.6	4.3
Stage 2-3	-3.7	2.7	-0.9	-1.9	-2.8	1.5	-5.5	8.3	-3.3
Stage 1-3	14.2	-9.5	3.4	11.7	-9.7	5.8	16.7	-9.4	1.0

according to the location and orientation of the mitral and aortic valve annuli (**Fig.6**). Note that the three stages of the procedure are colour-coded using red, green and blue, which correspond to the stage 1- prior to minithoracotomy, stage 2 - following minithoracotomy, and stage 2 - post GUCI attachment, respectively.

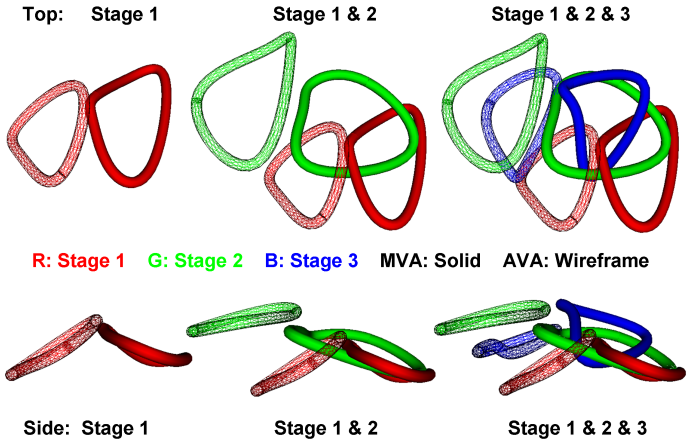

Figure 5. Figure showing the mitral (solid ring) and aortic (wireframe ring) valve annuli at different stages of the GUCI-based intracardiac procedure workflow in a porcine subject: stage 1 - before chest opening (red); stage 2 - after chest opening (green); stage 3 - after GUCI attachment (blue).

The movement of the heart during the robot-assisted CABG procedure from stage 1 (anesthetized, dual-lung ventilation) to stage 2 (single-lung ventilation) averaged to $\sim$ 24 mm for the mitral valve and $\sim$ 32.7 mm for the aortic; from stage 1 to stage 3 (chest wall insufflation), the mitral valve experienced a movement of $\sim$ 30 mm and the aortic movement averaged to $\sim$ 34 mm. **Table 2** provides a summary of the valvular displacements with respect to the L/R, A/P and S/I axes across the patients observed.

Moreover, **Fig. 7** shows the position of the mitral (solid ring) and aortic (wireframe ring) valve annuli colour-coded according to the three stages of the procedure.

For a better interpretation of the overall heart movement, in **Fig. 8** we displayed a surface model of the heart consisting of the left ventricle (shown as solid surface) and left atrium and aorta (shown and wireframe) at the three stages of the procedure: dual-lung ventilation shown in red, single-lung ventilation shown in green, and post chest insufflation, shown in blue.

3.2 Morphological Feature Characterization

Morphological changes of the annuli themselves were also assessed. Using principal component analysis and eigenvalue decomposition, we identified an orthonormal basis corresponding to each annulus; the eigenvectors corresponding to the largest and second largest eigenvalues were the principal in-plane orientations of the annulus,

Downloaded From: http://spiedigitallibrary.org/ on 12/17/2012 Terms of Use: http://spiedl.org/terms

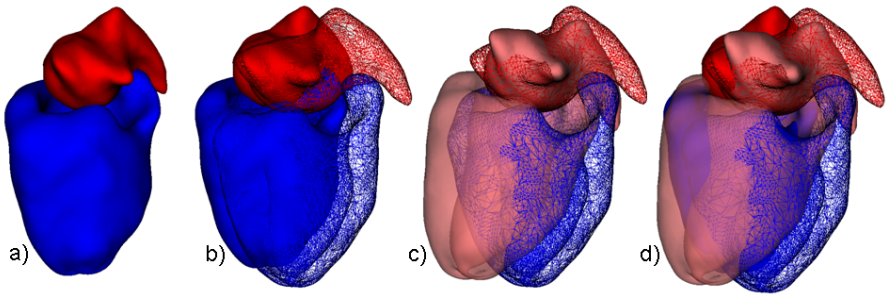

Figure 6. Global porcine heart orientation (left ventricle and left atrium models shown) throughout the peri-operative workflow associated with the off-pump GUCI-based intracardiac interventions on porcine subjects: a) Before opening chest; b) Before (surfaces) and after (wireframe) performing minithoracotomy; c) After minithoracotomy (wireframe) and after GUCI attachment (light-coloured surface); d) All-in-one generic pre-operative shift.

Table 2. Summary of the overall heart and valve displacement between consecutive stages during off-pump robot-assisted CABG interventions based on $N = 4$ patients; Stage 1: dual-lung ventilation; Stage 2: Single-lung ventilation; Stage 3: Chest insufflation. Note that displacements are reported according to the left/right (L/R), anterior/posterior (A/P) and superior/inferior (S/I) directions, where positive displacements are measured toward the right, anterior and superior direction, respectively.

Workflow Stage	**Overall Heart**			**Mitral Valve**			**Aortic Valve**		
	L/R	**A/P**	**S/I**	**L/R**	**A/P**	**S/I**	**L/R**	**A/P**	**S/I**
Stage 1-2	2.3	- 6.4	7.1	1.9	-1.6	6.8	2.6	-11.5	7.3
Stage 2-3	15.3	-2.7	-7.4	16.2	-2.6	-7.8	14.5	-2.8	-6.9
Stage 1-3	17.6	-9.0	-0.4	18.1	-4.2	-1.0	17.2	-13.9	0.4

while the smallest eigenvector corresponded to the unit normal vector describing its orientation, as shown in (**Fig.4**).

We also estimated the effective perimeter of the mitral and aortic annuli, as well as the distance between the two valves at each stage in both the GUCI-based porcine procedures and the robot-assisted CABG interventions. These parameters represent a measure of the morphology of the features of interest and according to their

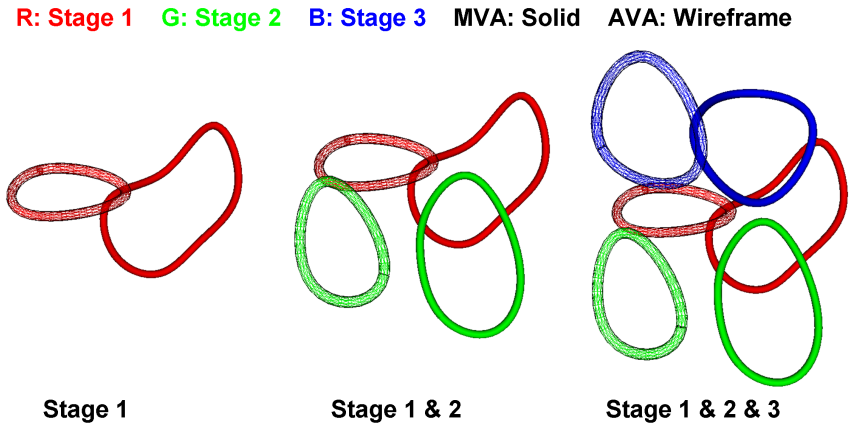

Figure 7. Figure showing the mitral (solid ring) and aortic (wireframe ring) valve annuli at different stages of the robot-assisted CABG procedure workflow in a patient: stage 1 - dual-lung ventilation (red); stage 2 - single-lung ventilation (green); stage 3 - chest insufflation (blue).

Downloaded From: http://spiedigitallibrary.org/ on 12/17/2012 Terms of Use: http://spiedl.org/terms

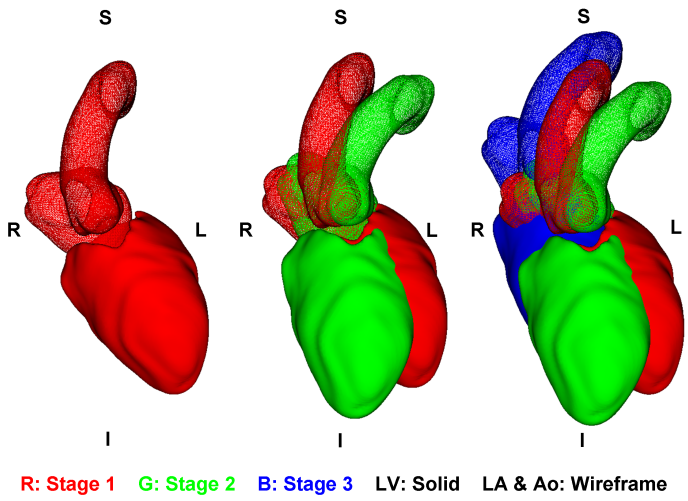

Figure 8. Figure showing the global displacement of the heart at the three different stages associated with the robot-assisted CABG procedure. Left ventricle (solid surface) and left atrium and aorta (wireframe) are shown th red, green and blue at the three workflow stages.

Table 3. Characterization of the mitral (MVA) and aortic valve (AVA) annuli during the peri-operative workflow of the GUCI-based off-pump procedures for $N = 2$ porcine subjects: effective perimeter (Length), effective major (MjA) and minor axes (MiA), inter-annular distance (mm) and inter-annular angle (deg).

Workflow Stage	Mitral Annulus (MVA)			Aortic Annulus (AVA)			Annular Distance	Annular Angle
	Length	MjA	MiA	Length	MjA	MiA		
Pre-operative	103.4	11.9	9.0	68.2	8.1	7.1	23.8	52
Before Incision	103.2	9.4	8.5	81.2	10.9	7.2	22.5	52
After Incision	109.4	14.4	8.9	107.8	11.1	8.9	26.4	39
After GUCI	88.0	12.2	6.8	87.8	10.0	8.2	22.3	45

variability across the procedural workflow, one can determine whether significant local deformations are induced and whether a rigid-body registration approach is sufficient. A summary of these results is included in **Table 3** for the GUCI-based porcine interventions and in **Table 4** for the robot-assisted CABG procedures.

Table 4. Characterization of the mitral (MVA) and aortic valve (AVA) annuli during the peri-operative workflow of the off-pump robot-assisted CABG procedures based on $N = 4$ patients: effective perimeter (Length), effective major (MjA) and minor axis (MiA), inter-annular distance (mm) and inter-annular angle (deg).

Workflow Stage	Mitral Annulus (MVA)			Aortic Annulus (AVA)			Annular Distance	Annular Angle
	Length	MjA	MiA	Length	MjA	MiA		
Dual-lung Vent.	133.8	16.9	10.8	97.4	12.8	8.8	31.5	49
Single-lung Vent.	123.4	14.9	11.6	82.8	10.6	8.0	33.4	46
Chest Insufflation	123.2	14.6	10.9	106.0	12.5	7.2	31.5	75

4. DISCUSSION

The main focus of this work was to explore the displacement of the heart and features of interest within the heart during the peri-operative workflow of minimally invasive cardiac interventions. This work was in fact motivated by our on-going developments on the model-enhanced surgical guidance environment and its application in

Downloaded From: http://spiedigitallibrary.org/ on 12/17/2012 Terms of Use: http://spiedl.org/terms

off-pump intracardiac intervention, where intracardiac access is achieved via the Guiraudon Universal Cardiac Introducer. This novel therapy technique requires the registration of pre-operative images and models to the intra-operative US imaging environment, a process which involves features of interest that may undergo both location as well as morphological changes during the procedure workflow. We also extended this work toward a different application which was initiated by the need to update a pre-operative surgical plan according to changes induced during the peri-operative workflow. As such, we have used similar technique to estimate the location of the features of interest and the heart overall at different stages during the procedure and also evaluate the morphological variations of these features across the peri-operative workflow.

In the context of our original motivation — the GUCI-based off-pump intracardiac interventions — it appears that the porcine heart undergoes an overall movement of under 15 mm in the lateral direction followed by a $\sim$ 9 mm movement in the anterior/posterior direction and a $\sim$ 3 mm movement in the superior/inferior direction between the initial peri-operative stage and the GUCI attachment. These changes are sufficiently large to require the model-to-subject registration to be performed just before therapy delivery, and therefore after GUCI attachment and surgical tool insertion.

In the context of the robot-assisted CABG procedures, we have currently analyzed the data from 4 patients from a total of over 50 patients who have agreed to participate in the study. Similarly, we have noticed substantial movement of the heart and valvular structures caused by the lung deflation and chest insufflation. The overall heart displacement was on the order of 17 mm and 9 mm in the lateral and anterior/posterior direction, respectively, while the superior/inferior displacement was on the order of 2 mm.

The morphological characterization of the mitral and aortic valve annuli has also revealed small variations in the effective perimeter and effective length of the major and minor axes of the valvular structures between the three stages for both types of procedure under investigation. Using the GraphPad Prism 4 statistical analysis package, we have performed a statistical comparison using a two-way analysis of variance (ANOVA) between the effective perimeter and effective long and short axes of the mitral and aortic annuli across the patient sample. The result have shown that no significant differences ($p > 0.05$) existed between these parameters at different procedure stage, except for those due to the patient variability, such as the size of the patients and their organs. Moreover, no significant differences were observed in the inter-annular distance ($p > 0.1$). These two observations together suggest that no significant morphological changes have occurred during the procedure workflow and therefore a rigid body registration may be sufficient to either update the pre-operative surgical plan for robot-assisted CABG procedures, or to perform the model-to-subject registration for the GUCI-based model-enhanced US guided procedures.

While this method is suitable to evaluate the changes in position of the heart and features on interest, we have nevertheless identified several challenges with respect to both data acquisition and post-processing. The peri-operatvie US images are acquired using a magnetically tracked transducer and the acquisition is gated to the ECG signal of the subject. For the porcine subjects the ECG gating was more consistent thanks to a better control of the heart rate compared to the patients. Moreover, we have also observed small interference between the unshielded ECG leads and the tracking system, issue which will be addressed by using better shielded leads. However, the heart rate variability observed in the patients leads to the major concern in the image acquisition: the patients undergoing these procedures suffer from various medical conditions which lead to inconsistent heart rate and also prevent the administration of heart-rate controlling medication to the extent required for "clean" image acquisition. As such, the ECG trigger, although set for diastole, may actually trigger later in the cardiac cycle, leading to a systolic image acquisition and therefore different position and orientation of the features of interest. This issue related to the heart-rate variability in patients needs to be addressed at the software level.

Another challenge arises due to the large degree of "manuality" currently involved in the post-processing of the data. All peri-operative images are accessed by the clinician off-line and the features of interest are segmented manually. In spite of manual segmentation being the clinical gold-standard procedure, we believe that there is an inherent degree of variability associated with the feature identification process, which, in turn, will affect the shape, position and orientation of the segmented features. To date we have not yet assessed the variability of the feature identification, but we plan to use the morphological characterization parameters to evaluate the repeatability and reproducibility of the segmentation as performed by different clinicians at different time points.

Downloaded From: http://spiedigitallibrary.org/ on 12/17/2012 Terms of Use: http://spiedl.org/terms

5. CONCLUSIONS AND FUTURE WORK

Motivated by the well-known fact that pre-operative information can finitely depict the intra-operative cardiac anatomy and morphology, this work presents an analysis of the changes in location of the heart and the variations in morphology of features of interest arising during the workflow of minimally invasive procedures. Here we have estimated the global heart displacement and morphological characteristics of the mitral and aortic valve annuli in two types of minimally invasive procedures. This information is not only critical to assess anatomical differences induced during the procedure itself, but it is also crucial to update a pre-operative plan by including the peri-operative changes in order to better suit the intra-operative guidance environment. In terms of out GUCI-based model-enhanced US guidance interventions, this work allows us to estimate the effect of the procedure workflow on the model-to-patient registration, and suggest the necessity to update the registration prior to therapy delivery. The work presented here is still in its infancy and we expect to have a more robust evaluation of the overall heart displacement associated with the robot-assisted CABG procedure once more patient data becomes available and some of the challenges associated with the ECG-gated image acquisition are addressed.

ACKNOWLEDGMENTS

The authors thank Dr. Usaf Aladl, Dr. Andrew Wiles and Jaques Milner for their support, Dr. Gérard M. Guiraudon and Dr. Doug Jones for their clinical expertise, and Sheri Van Lingen for assistance with animal support. In addition, we would like to acknowledge funding for this work provided by the Natural Sciences and Engineering Research Council, Canadian Institutes of Health Research, Heart and Stroke Foundation of Canada, Ontario Research Fund, Ontario Innovation Trust, and Canadian Foundation for Innovation.

REFERENCES

[1] Modi, P., Hassan, A., and Chitwood, W. R. J., "Minimally invasive mitral valve surgery: a systematic review and meta-analysis," *Eur J Cardiothorac Surg.* **34**, 943–52 (2008).

[2] Dotty, D. B., Flores, J. H., and Doty, J. R., "Cardiac valve operations using a partial sternotomy technique," *J Card Surg.* **15**, 35–42 (2000).

[3] Vassiliades, T. A., Block, P. C., and Cohn, L. H., "The clinical development of percutaneous heart valve technology," *J Thorac Cardiovasc Surg.* **129**, 970–76 (2005).

[4] Lutter, G., Ardehali, R., Cremer, J., and Bonhoeffer, P., "Percutaneous valve replacement: current state and future prospects," *Ann Thor Surg.* **78**, 2199–2206 (2004).

[5] Modi, P., Rodriguez, E., and Chitwood, W. R. J., "Robot-assisted cardiac surgery," *Interact Cardiovasc Thorac Surg.* **9**, 500–5 (2009).

[6] Guiraudon, G., Jones, D., Bainbridge, D., and Peters, T., "Mitral valve implantation using off-pump closed beating intracardiac surgery: a feasability study," *Interact Cardiovasc Thorac Surg.* **6**, 603–607 (2007).

[7] Linte, C. A., Moore, J., and Wedlake, C. *et al.*., "Inside the beating heart: An *in vivo* feasibility study on fusing pre- and intra-operative imaging for minimally invasive therapy," *Int J CARS* **4**, 113–122 (2009).

[8] Ma, Y. L., Penney, G. P., Rinaldi, C. A., Cooklin, M., Razavi, R., and Rhode, K. S., "Echocardiography to magnetic resonance image registration for use in image-guided cardiac catheterization procedures," *Phys Med Biol.* **54**, 5039–55 (2009).

[9] Wierzbicki, M., Drangova, M., Guiraudon, G. M., and Peters, T. M., "Validation of dynamic heart models obtained using non-linear registration for virtual reality training, planning, and guidance of minimally invasive cardiac surgeries," *Med Image Anal.* **8**, 387–401 (2004).

[10] Lorensen, W. E. and Cline, H. E., "Marching cubes: A high resolution 3d surface construction algorithm," *Computer Graphics* **21** (1987).

[11] Gobbi, D. G., Comeau, R. M., and Peters, T. M., "Ultrasound probe tracking for real-time ultrasound/MRI overlay and visualization of brain shift," in [*Lect Notes Comput Sci.*], *Proc. MICCAI* **1679**, 920–27 (2008).

[12] Wiles, A. D., Linte, C. A., and Moore, J. *et al.*., "Object identification accuracy under ultrasound enhanced virtual reality for minimally invasive cardiac surgery," *Proc. of SPIE.* **6918**, 69180E–12 (2008).

Downloaded From: http://spiedigitallibrary.org/ on 12/17/2012 Terms of Use: http://spiedl.org/terms